Accepted Manuscript

Magnetic structures in TmPdIn and TmAgSn

S. Baran, A. Szytuła, D. Kaczorowski, F. Damay

PII: S0925-8388(15)31757-6

DOI: 10.1016/j.jallcom.2015.11.200

Reference: JALCOM 36055

To appear in: *Journal of Alloys and Compounds*

Received Date: 21 August 2015

Revised Date: 30 October 2015

Accepted Date: 25 November 2015

Please cite this article as: S. Baran, A. Szytuła, D. Kaczorowski, F. Damay, Magnetic structures in TmPdIn and TmAgSn, *Journal of Alloys and Compounds* (2015), doi: 10.1016/j.jallcom.2015.11.200.

Magnetic structures in TmPdIn and TmAgSn

S. Baran[a,*], A. Szytuła[a], D. Kaczorowski[b], F. Damay[c]

[a] *M. Smoluchowski Institute of Physics, Jagiellonian University, prof. Stanisława Łojasiewicza 11, PL-30-348 Kraków, Poland*
[b] *Institute of Low Temperature and Structure Research, Polish Academy of Sciences, P. O. Box 1410, PL-50 950 Wrocław, Poland*
[c] *Laboratoire Léon Brillouin, CEA-CNRS UMR 12, F-91191 Gif-sur-Yvette Cedex, France*

Abstract

Low temperature antiferromagnetic structures of TmPdIn and TmAgSn have been derived from powder neutron diffraction data. The magnetic structure of TmPdIn is a commensurate one and related to a propagation vector $\vec{k} = [\frac{1}{3}, \frac{1}{3}, \frac{1}{2}]$ while the incommensurate sine-modulated structure of TmAgSn is connected with $\vec{k} = [k_x, -k_x, 0]$ where $k_x = 0.1314(2)$. The thulium magnetic moments are constrained within the basal plane and show 'triangular' arrangement. Validity of obtained magnetic structures is discussed on the basis of symmetry analysis.

Keywords:
intermetallics, rare earth alloys and compounds, magentisation, phase transitions, neutron diffraction

1. Introduction

Equiatomic intermetallics RTX, where R is a rare earth element, T – d-electron metal and X – p-electron element, have been intensively investigated with respect to their crystal chemistry and physical properties [1, 2]. In these compounds, the rare earth magnetic moments order antiferromagnetically at low temperatures.

TmPdIn and TmAgSn, investigated in this work, crystallize at room temperature in a hexagonal crystal structure of the ZrNiAl-type [3, 4, 5]. Previously reported magnetic and specific heat data indicated antiferromagnetic ordering below the Néel temperature $T_N = 2.7$ K in TmPdIn [6, 7] and 4.2 K in TmAgSn [8], while the paper by Sebastian et al. reports no magnetic ordering in TmAgSn down to 2 K [4].

In this work, crystal and magnetic structures of TmPdIn and TmAgSn are investigated by means of neutron diffraction. It is a part of systematic study of magnetic structures in thulium ternary intermetallics of general composition TmTX. The compounds are investigated in order to determine influence of surroundings atoms on magnetic order. Up to now, antiferromagnetic ordering has been found in TmNiIn [9], TmPtIn [10], TmAgGe [11] and TmAgSi [12] below the critical temperature of 2.5 K, 3.5 K, 4.2 K and 3.3 K, respectively. Complex magnetic structures have been determined in all these compounds. As bulk measurements reported up to now for TmPdIn [6, 7] and TmAgSn [8] cannot provide detailed information on magnetic structures, the neutron diffraction data are reported in this work.

*Corresponding author. Phone: (+48 12) 6644686; e-mail: stanislaw.baran@uj.edu.pl

2. Experimental details

Polycrystalline samples of TmPdIn and TmAgSn were prepared by arc melting constituent metals, with all stated purity better than 99.9 wt %, under ultra-pure argon atmosphere. Subsequently, the samples were wrapped in tantalum foil, sealed in an evacuated silica tube and heat treated at 973 K for 10 days. Quality of the samples were checked by X-ray powder diffraction (XRD) at room temperature on an X'Pert PRO PANalytical diffractometer with CuK_α radiation. The X-ray diffraction data are analyzed in Refs. [6, 8].

Powder neutron diffraction patterns were collected at temperatures ranging from 1.8 to 8.0 K on the G4.1 diffractometer installed at the Orphée reactor (Laboratoire Léon Brillouin, CEA-CNRS Saclay, France). The incident neutron wavelength was 2.426 Å.

The obtained X-ray and neutron diffraction patterns were analyzed using the computer program *FullProf* [13]. Symmetry analysis was performed with the use of the computer program *basireps* distributed together with *FullProf*.

3. Crystal structure

The X-ray diffraction data collected at room temperature as well as the neutron diffraction data indicate that the investigated samples have the ZrNiAl-type crystal structure with the lattice parameters being in agreement with literature data [3, 4, 5].

Fig. 1 shows neutron diffraction patterns taken at paramagnetic state at 6.0 K and 8.0 K for TmPdIn (Fig. 1a) and TmAgSn (Fig. 1b), respectively, together with calculated profiles obtained by Rietveld refinement method. Both patterns indicate presence of weak reflections that cannot be indexed within the main TmTX phases. Limited number of these low intensity reflections made identification of impurity phases impossible.

Table 1 contains crystal structure information based on the best Rietveld fits to the neutron diffraction data.

Table 1: Structural parameters of TmPdIn and TmAgSn refined from the neutron diffraction data collected at 6.0 K (TmPdIn) or 8.0 K (TmAgSn), and corresponding reliability factors.

	TmPdIn	TmAgSn
Crystal structure	ZrNiAl-type	
Space group	$P\bar{6}2m$ (No. 189)	
T [K]	6.0	8.0
a [Å]	7.617(2)	7.242(1)
c [Å]	3.706(1)	4.422(1)
c/a	0.4865(2)	0.6106(2)
V [Å^3]	186.21(9)	200.85(7)
Tm at 3(g)	$(x_{Tm}, 0, \frac{1}{2})$ $(0, x_{Tm}, \frac{1}{2})$ $(\bar{x}_{Tm}, \bar{x}_{Tm}, \frac{1}{2})$	
x_{Tm}	0.592(2)	0.570(2)
In or Ag at 3(f)	$(x, 0, 0)$ $(0, x, 0)$ $(\bar{x}, \bar{x}, 0)$	
x_{In} or x_{Ag}	0.264(4)	0.236(4)
Pd or Sn at 1(b)	$(0, 0, \frac{1}{2})$	
Pd or Sn at 2(c)	$(\frac{1}{3}, \frac{2}{3}, 0)$ $(\frac{2}{3}, \frac{1}{3}, 0)$	
$R_{profile}$ [%]	3.23	2.61
R_{Bragg} [%]	10.2	3.60
χ^2 [%]	1.66	2.01

4. Magnetic structure

The neutron diffraction patterns collected below the respective Néel temperatures for TmPdIn and TmAgSn show presence of additional Bragg reflections of magnetic origin (Figs. 2a and 3a, respectively).

In order to facilitate determination of the magnetic structures of both compounds a symmetry analysis was performed. The symmetry analysis method is based on the theory of representation of space groups formulated and developed by Bertaut [14] and Izyumov and Syromyatnikov [15]. A magnetic structure, as an axial vector function $\vec{S}^{\{\vec{k}_L\}}$ localised on the set of equivalent positions of a given space group, may be presented as a linear combination of basic vectors $\vec{\Psi}^{\{\vec{k}_L\}}_{\nu,\lambda}$ of irreducible representations of this space group

$$\vec{S}^{\{\vec{k}_L\}} = \sum_{L=1}^{l_{\vec{k}}} \sum_{\nu=1}^{j} \sum_{\lambda=1}^{l_\nu} C^{\{\vec{k}_L\}}_{\nu,\lambda} \vec{\Psi}^{\{\vec{k}_L\}}_{\nu,\lambda} \quad (1)$$

where L labels arms of the star for a given propagation vector $\vec{k}_L$, ν labels irreducible representations, λ labels dimensions of a particular irreducible representation while $C^{\{\vec{k}_L\}}_{\nu,\lambda}$ are the coefficients which have to be determined from refinement of the experimental data. The form of $\vec{\Psi}^{\{\vec{k}_L\}}_{\nu,\lambda}$ follows the theory of group and representations.

4.1. TmPdIn

A differential neutron diffraction pattern of TmPdIn, showing magnetic contribution only, has been derived (Fig. 2a) by subtracting the paramagnetic data collected at 8.0 K from the pattern taken at 2.0 K. The positions of Bragg reflections of magnetic origin lead to a propagation vector $\vec{k} = [\frac{1}{3}, \frac{1}{3}, \frac{1}{2}]$ which is the only vector of the star. Despite $-\vec{k}$ is not equivalent to $\vec{k}$ nor belongs to the star it has to be taken into account in calculations in order to obtain real components of the magnetic structure.

The elementary unit cell contains three rare-earth atoms at 3(g) site which occupy the following positions:

Tm$_1$ atom at $x_{Tm}, 0, \frac{1}{2}$
Tm$_2$ atom at $0, x_{Tm}, \frac{1}{2}$
Tm$_3$ atom at $1 - x_{Tm}, 1 - x_{Tm}, \frac{1}{2}$

where the values of x_{Tm} are listed in Table 1. In case of the space group $P\bar{6}2m$ and the propagation vector $\vec{k} = [\frac{1}{3}, \frac{1}{3}, \frac{1}{2}]$ these three atoms belong to one orbit which means that their magnetic moment components are related to each other by symmetry operations. Thus symmetry imposes constraints to magnetic moments directions and their magnitudes.

For the above mentioned space group, propagation vector and 3(g) site, theory predicts: three one-dimensional irreducible representations τ_1, τ_2 and τ_3, each of them appearing once, one two-dimensional irreducible representation τ_5 appearing once and one two-dimensional irreducible representation τ_6 appearing twice (the names of representations follow the output of *basireps*). Refinement of the neutron diffraction data show unambiguously that the magnetic structure of TmPdIn is related to the basic vectors of τ_6, so only this representation will be taken into account in what follows.

Table 2: Basic vectors of the irreducible representation τ_6 as calculated by the *basireps* computer program for the space group $P\bar{6}2m$, propagation vector $\vec{k} = [\frac{1}{3}, \frac{1}{3}, \frac{1}{2}]$ and site 3(g). As vector components are generally complex numbers the real and imaginary parts are listed in separate rows.

		Tm$_1$	Tm$_2$	Tm$_3$
$\vec{\Psi}_1$	Re	[1, 0, 0]	[0, -0.5, 0]	[0.5, 0.5, 0]
	Im	[0, 0, 0]	[0, -0.87, 0]	[0.87, 0.87, 0]
$\vec{\Psi}_2$	Re	[0, 1, 0]	[0.5, 0.5, 0]	[-0.5, 0, 0]
	Im	[0, 0, 0]	[0.87, 0.87, 0]	[-0.87, 0, 0]
$\vec{\Psi}_3$	Re	[0.5, 0, 0]	[0, -1, 0]	[-0.5, -0.5, 0]
	Im	[0.87, 0, 0]	[0, 0, 0]	[-0.87, -0.87, 0]
$\vec{\Psi}_4$	Re	[-0.5, -0.5, 0]	[-1, 0, 0]	[0, 0.5, 0]
	Im	[-0.87, -0.87, 0]	[0, 0, 0]	[0, 0.87, 0]

The basic vectors of τ_6 are listed in Table 2. Thus, the magnetic structure of TmPdIn can be expressed in the following form:

$$\vec{S}(\mathrm{Tm}_1) = [u + \tfrac{1}{2}w - \tfrac{1}{2}p, v - \tfrac{1}{2}p, 0] + 0.87i[w - p, -p, 0]$$
$$\vec{S}(\mathrm{Tm}_2) = [\tfrac{1}{2}v - p, -\tfrac{1}{2}u + \tfrac{1}{2}v - w, 0] + 0.87i[v, -u + v, 0]$$
$$\vec{S}(\mathrm{Tm}_3) = (\tfrac{1}{2} + 0.87i)[u - v - w, u - w + p, 0] =$$
$$= [u - v - w, u - w + p, 0] \exp(2\pi i 0.1667)$$

where u, v, w and p are the $C_{\nu,\lambda}^{\{\vec{k}_L\}}$ constants from Equation 1. The best fit to the experimental data has been obtained for $u \neq 0, v = w = p = 0$ or alternatively $w \neq 0, u = v = p = 0$. Both the solutions lead to the same physical magnetic structure thus only the first one is further analyzed. While assuming $u \neq 0, v = w = p = 0$, the TmPdIn magnetic structure may be reduced to:

$$\vec{S}(\mathrm{Tm}_1) = [u, 0, 0]$$
$$\vec{S}(\mathrm{Tm}_2) = (\tfrac{1}{2} + 0.87i)[0, -u, 0] = [0, -u, 0]\exp(2\pi i 0.1667)$$
$$\vec{S}(\mathrm{Tm}_3) = (\tfrac{1}{2} + 0.87i)[u, u, 0] = [u, u, 0]\exp(2\pi i 0.1667)$$

The above magnetic structure description does not define real magnetic structure unambiguously due to known *diffraction phase problem*. A Bragg reflection intensity is proportional to a square of absolute value of structure factor, hence multiplying structure factor by a factor of general form $e^{i\phi}$ does not influence calculated diffraction pattern and the number ϕ, called in this context *magnetic phase*, has to be evaluated independently in order to provide physically valid magnetic structure model.

In the discussed case, it is not possible to get the same value of magnetic moment for all thulium atoms. However, for $\phi = \frac{1}{4}$ (in units of 2π) one gets the magnetic moment equal to either 6.15(7) μ_B or zero. Fig. 2b shows such a structure together with comparison of the experimental and calculated diffraction patterns (while calculating real magnetic structure both the $\vec{k}$ and $-\vec{k}$ propagation vetors were taken into account in order to eliminate imaginary components of the magnetic moments). The refined parameters of the magnetic structure are gathered in Table 3.

Table 3: Magnetic structure parameters of TmPdIn and TmAgSn refined from the neutron diffraction data collected at 2.0 K (TmPdIn) or 2.7 K (TmAgSn), and corresponding reliability factors. μ_A denotes amplitude of modulation while μ denotes magnetic moment on particular Tm atom in case of the commensurate magnetic structure of TmPdIn or an average magnetic moment, calculated as $\frac{2\mu_A}{\pi}$, in case of the incommensurate magnetic structure of TmAgSn.

	TmPdIn	TmAgSn
T [K]	2.0	2.7
$\vec{k}$	$[\frac{1}{3}, \frac{1}{3}, \frac{1}{2}]$	[0.1314(2),-0.1314(2),0]
μ_A [μ_B]	7.10(8)	8.50(9)
μ [μ_B]	6.15(7) or 0	5.41(6)
	Direction of magnetic moment	
Tm_1	[100]	
Tm_2	[010]	
Tm_3	[110]	
$R_{profile}$ [%]	3.79	4.47
$R_{magnetic}$ [%]	6.52	8.76
χ^2 [%]	1.91	3.63

4.2. TmAgSn

A differential neutron diffraction pattern of TmAgSn derived as a difference between the pattern collected at 2.7 K and the paramagnetic one taken at 8.0 K is shown in Fig. 3a. The Bragg reflections of magnetic origin may be indexed with a propagation vector $\vec{k} = [0.1314(2), 0, 0]$. $\vec{k}$ and $-\vec{k}$ are not equivalent but both belong to the star formed by 6 vectors, namely: $[k_x, 0, 0]$, $[0, -k_x, 0]$, $[0, k_x, 0]$, $[-k_x, k_x, 0]$, $[-k_x, 0, 0]$ and $[k_x, -k_x, 0]$, where $k_x = 0.1314(2)$.

In the case of the space group $P\bar{6}2m$ and the propagation vector $\vec{k} = [0.1314(2), 0, 0]$, the set of $3(g)$ equivalent positions splits on three independent orbits, each of them containing one Tm atom. The symmetry analysis allows for these constraints only two one-dimensional irreducible representations, τ_1 and τ_2, the first one appearing once while the second one twice. τ_1 has its basic vector perpendicular to the basal plane while the basics vectors of τ_2 lie within the basal plane. As a result, from the point of view of symmetry analysis, the magnetic moment related to particular orbit may take any direction and magnitude regardless the directions and magnitudes of the magnetic moments connected with two remaining orbits. Thus, in this very special case, symmetry does not impose any restrictions or constraints to the magnetic structure.

The best fit to the experimental data has been found for a sine-modulated magnetic structure with magnetic moments oriented along the [100], [010] and [110] directions for Tm_1, Tm_2 and Tm_3, respectively. Similar fit quality can be achieved with the use of any propagation vectors belonging to the k-star mentioned at the beginning of this subsection. In Fig. 3b, the structure obtained while assuming $\vec{k} = [0.1314(2), -0.1314(2), 0]$ is shown. The refined parameters and reliability factors are listed in Table 3.

For an incommensurate magnetic structure a global *magnetic phase* parameter has no significance as magnetic atom having any selected magnetic phase can be found regardless what the global *magnetic phase* is. However, relative phase shifts, defined as differences between magnetic phases of particular Tm atoms have physical meaning as they define magnetic couplings between magnetic moments located at different orbits. During the refinement, the magnetic phase shifts were fixed to $\phi_{13} = 0.56483$ and $\phi_{23} = 0.43517$ in units of 2π. These numbers correspond to $\phi_{i3} = \frac{1}{2} + \vec{k} \cdot \Delta\vec{r}_{i3}$, where $\Delta\vec{r}_{i3} = \vec{r}_i - \vec{r}_3$ is a difference between the position vectors of Tm_i and Tm_3.

5. Conclusions and Discussion

TmPdIn and TmAgSn have been found to order antiferromagnetically at low temperatures with the respective Néel temperatures of 2.7 K [6, 7] and 4.2 K [8]. The neutron diffraction data presented in this work confirm that magnetic moments are localized on the Tm^{3+} ion as it was previously found from magnetometric data [6, 7, 8]

The best fits to the neutron diffraction data indicate a commensurate magnetic structure related to a propagation vector $\vec{k} = [\frac{1}{3}, \frac{1}{3}, \frac{1}{2}]$ in TmPdIn and an incommensurate one connected with $\vec{k} = [0.1314(2), -0.1314(2), 0]$ in TmAgSn. In both cases the thulium magnetic moments are confined within the basal plane and show characteristic 'triangular' arrangement, meaning that their directions may differ by multiplicity

of $\frac{\pi}{3}$ (60^o). The triangular arrangement of magnetic moments in thulium intermetallics of the TmTX composition is quite common and has been found also in TmPtIn [10], TmAgGe [11] and TmAgSi [12]. This is an evidence of crystal electric field playing significant role in formation of magnetic structure in TmTX.

As the ZrNiAl-type crystal structure is a layered one the same feature characterizes the magnetic structures. The propagation vectors describing magnetic ordering in TmTX have always one or two non-zero components within the basal plane, while their z-component may be either zero or $\frac{1}{2}$. As a result, the magnetic structure consists of (001) layers which are coupled either ferro- ($k_z = 0$) or antiferromagnetically ($k_z = \frac{1}{2}$). Both commensurate and incommensurate structures are formed (see Table 4).

Table 4: Propagation vector describing antiferromagnetic structures in TmTX intermetallics.

	$\vec{k}$	Ref.
TmNiIn	$[0.281(2), 0.281(2), \frac{1}{2}]$	[9]
TmPtIn	$[\frac{1}{4}, \frac{1}{4}, \frac{1}{2}]$	[10]
TmAgGe	$[\frac{1}{2}, 0, 0], [-\frac{1}{2}, \frac{1}{2}, 0], [0, -\frac{1}{2}, 0]$	[11]
TmAgSi	$[\frac{1}{2}, 0, 0], [-\frac{1}{2}, \frac{1}{2}, 0], [0, -\frac{1}{2}, 0]$	[12]
TmPdIn	$[\frac{1}{3}, \frac{1}{3}, \frac{1}{2}]$	This work
TmAgSn	$[0.1314(2), -0.1314(2), 0]$	This work

It is worth noting that the neutron diffraction patterns collected below 2.0 K (TmPdIn) or 2.7 K (TmAgSn) contain a number of additional low intensity Bragg reflections. As they cannot be indexed within the main ZrNiAl-type crystal phase, they are probably related to magnetic structures of impurity phases mentioned in the section *Crystal structure*. Magnetic ordering in the impurity phases is presumably responsible for the anomalies in the ordered states of TmPdIn and TmAgSn observed in the magnetic and heat capacity data [6, 8].

Acknowledgements

S. Baran would like to thank LLB for kind hospitality during the time of neutron diffraction experiment.

References

[1] A. Szytuła, Crystal structures and magnetic properties of RTX rare earth intermetallics, Jagiellonian University Press, Kraków, 1998
[2] S. Gupta, K.G. Suresh, J. Alloys Comp. 618 (2015) 562–606, doi: 10.1016/j.jallcom.2014.08.079
[3] D. Mazzone, D. Rossi, R. Marazza, R. Ferro, J. Less Common Met. 80 (1981) P47–P52, doi: 10.1016/0022-5088(81)90100-4
[4] C.P. Sebastian, H. Eckert, C. Fehse, J.P. Wright, J.P. Attfield, D. Johrendt, S. Rayaprol, R.-D. Hoffmann, R. Pöttgen, J. Solid State Chem. 179 (2006) 2376–2385, doi: 10.1016/j.jssc.2006.04.038
[5] R. Ferro, R. Marazza, G. Rambaldi, Z. Metallkd. 65 (1974) 37–39
[6] D. Kaczorowski, A. Szytuła, Acta. Phys. Pol. A 127 (2015) 620-622, doi: 10.12693/APhysPolA.127.620
[7] D.X. Li, T. Yamamura, S. Nimori, K. Koyama, Y. Shiokawa, J. Alloys Comp. 418 (2006) 151–154, doi: doi:10.1016/j.jallcom.2005.07.081
[8] D. Kaczorowski, A. Szytuła, J. Alloys Comp. 615 (2014) 1–3, doi: 10.1016/j.jallcom.2014.06.153
[9] S. Baran, D. Kaczorowski, A. Arulraj, B. Penc, A. Szytuła, J. Magn. Magn. Mater. 323 (2011) 833–837, doi: 10.1016/j.jmmm.2010.11.028
[10] S. Baran, D. Kaczorowski, A. Arulraj, B. Penc, A. Szytuła, J. Magn. Magn. Mater. 322 (2010) 2177–2183, doi: 10.1016/j.jmmm.2010.02.005
[11] S. Baran, D. Kaczorowski, A. Arulraj, B. Penc, A. Szytuła, J. Magn. Magn. Mater. 321 (2009) 3256–3261, doi: 10.1016/j.jmmm.2009.05.064
[12] S. Baran, D. Kaczorowski, A. Hoser, B. Penc, A. Szytuła, J. Magn. Magn. Mater. 323 (2011) 222–225, doi: 10.1016/j.jmmm.2010.09.005
[13] J. Rodriguez-Carvajal, Physica B 192 (1993) 55–69, doi: 10.1016/0921-4526(93)90108-I
[14] E.F. Bertaut, J. Phys. Colloques 32 (C1) (1971) 462–470, doi: 10.1051/jphyscol:19711156
[15] Yu A. Izyumov, V. Syromyatnikov, Phase Transitions and Crystal Symmetry, Kluwer Scademic Publishers, Dordrecht, 1990 (Chapter 2)

Figure captions

Figure 1: Neutron diffraction patterns taken at paramgnetic state at 6.0 K (a) and 8.0 K (b) for TmPdIn and TmAgSn, respectively, together with Rietveld fit and difference plot. The vertical ticks indicate positions of Bragg reflections.

Figure 2: (a) Differential neutron diffraction patterns of TmPdIn together with Rietveld fit and difference plot. The pattern was constructed as a difference between experimental patterns collected at 2.0 K and 6.0 K. The vertical ticks indicate positions of the magnetic reflections. (b) Magnetic structure of TmPdIn (see the main text for details). The magnetic unit cell of TmPdIn consists of two such layers coupled antiferromagnetically one to another (due to the $\frac{1}{2}$ component of the propagation vector).

Figure 3: (a) Differential neutron diffraction patterns of TmAgSn together with Rietveld fit and difference plot. The pattern was constructed as a difference between experimental patterns collected at 2.7 K and 8.0 K. The vertical ticks indicate positions of the magnetic reflections. (b) Sine-modulated magnetic structure of TmAgSn obtained from refinement while assuming $\vec{k} = [k_x, -k_x, 0]$ where $k_x = 0.1314(2)$ (see the main text for details). The structure is an incommensurate one so the magnetic unit cell cannot be defined. Thus an area covering few crystal unit cell shown in order to get an idea how the structure looks like.

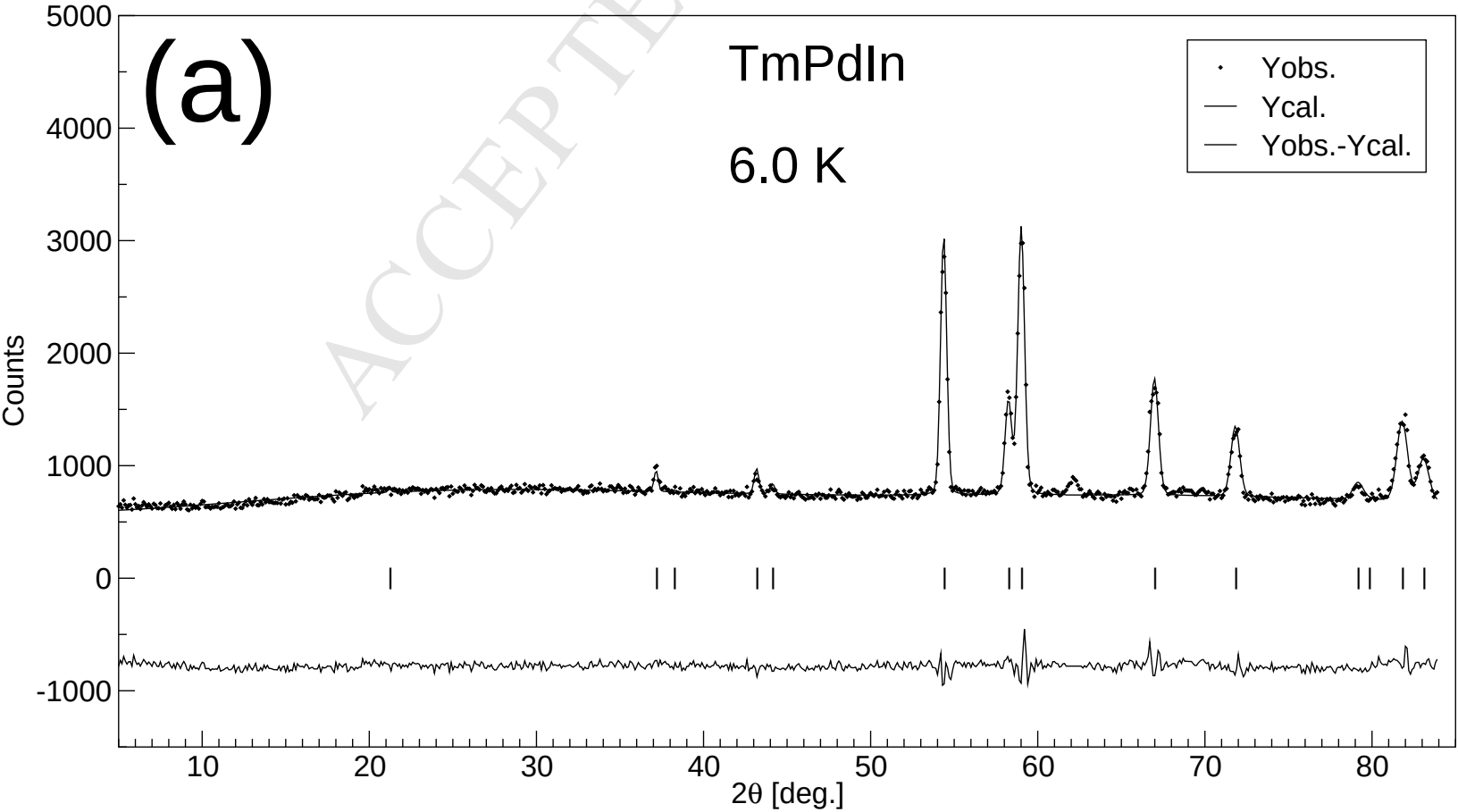

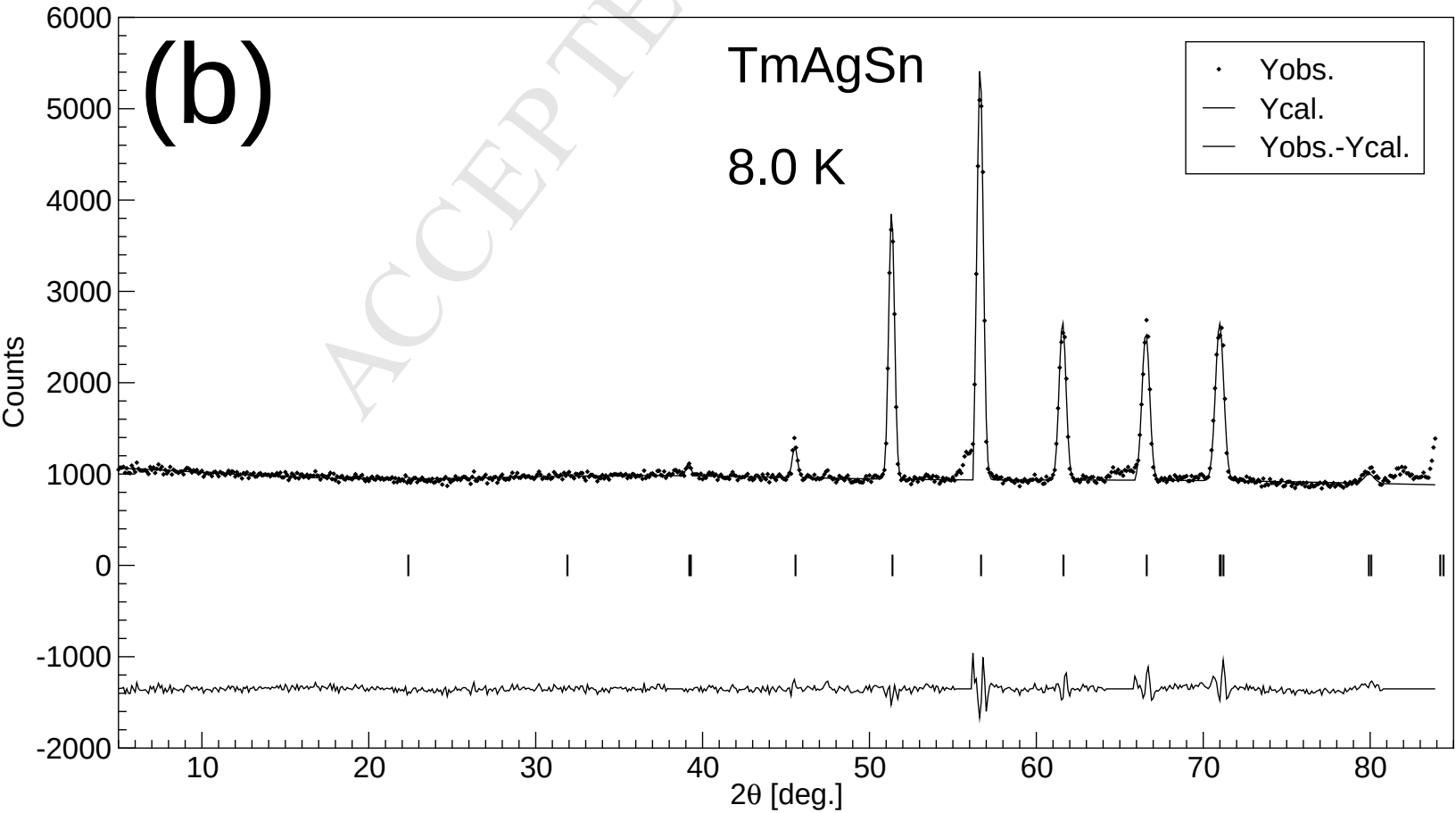

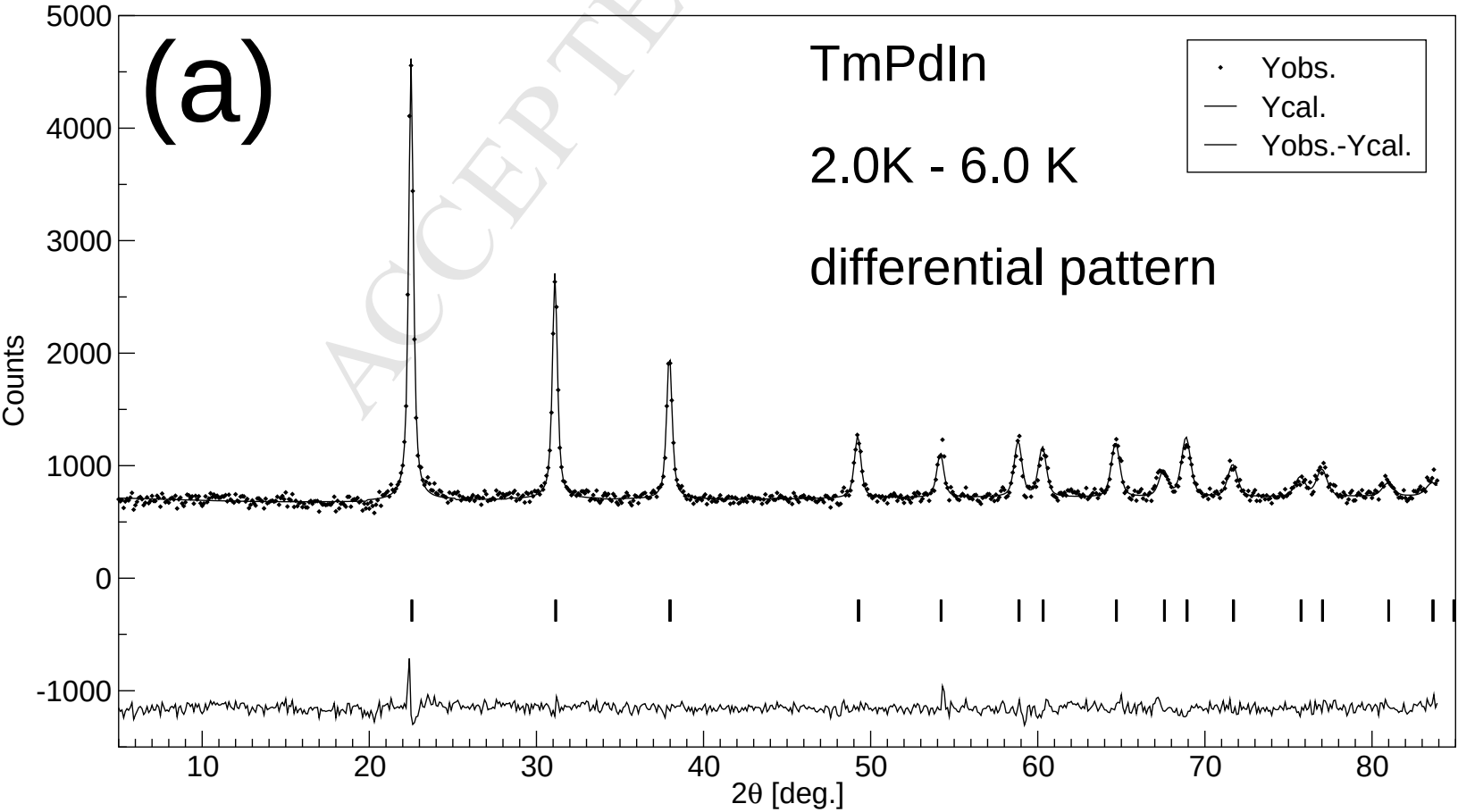

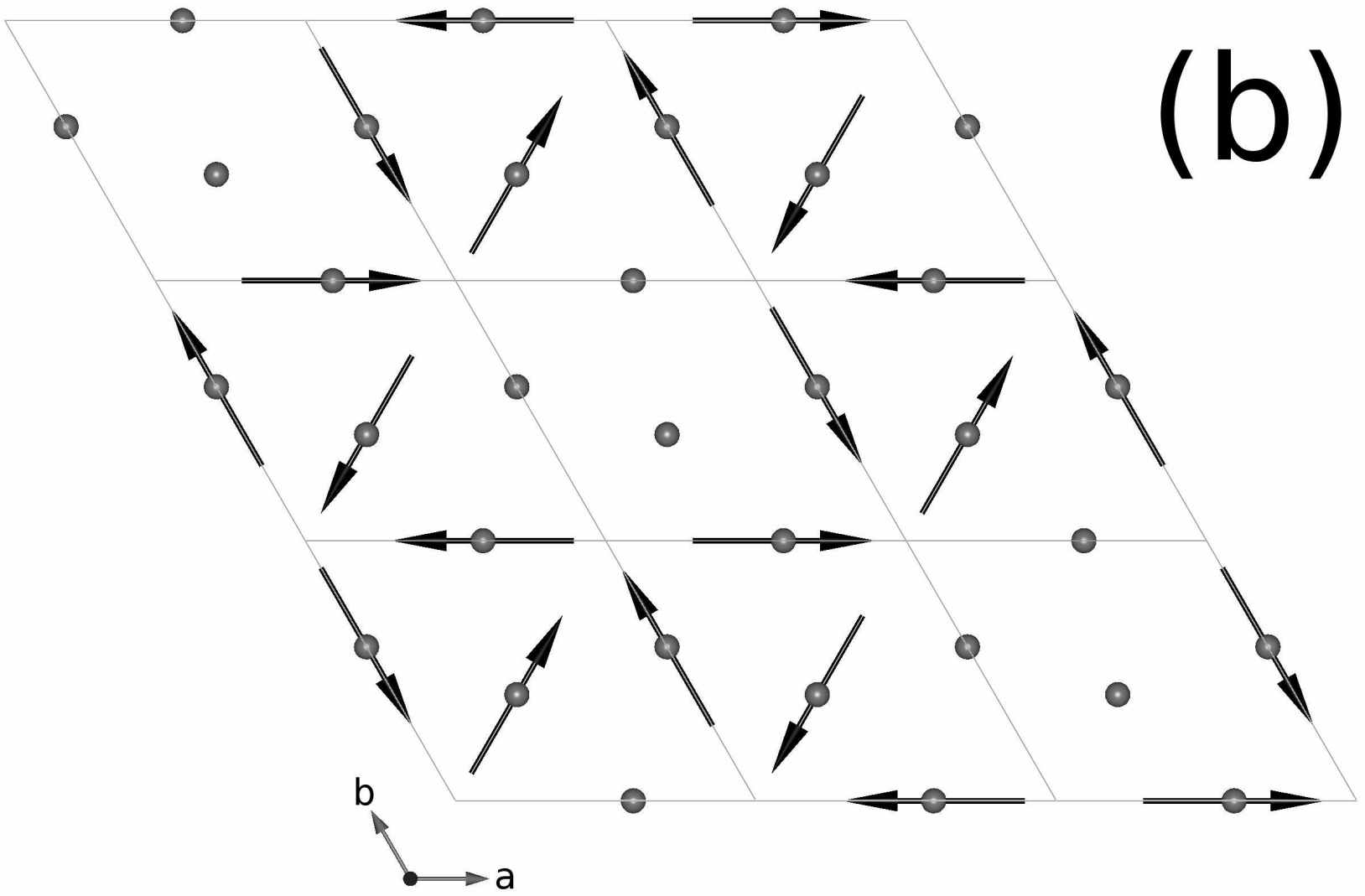
(b)
b
a

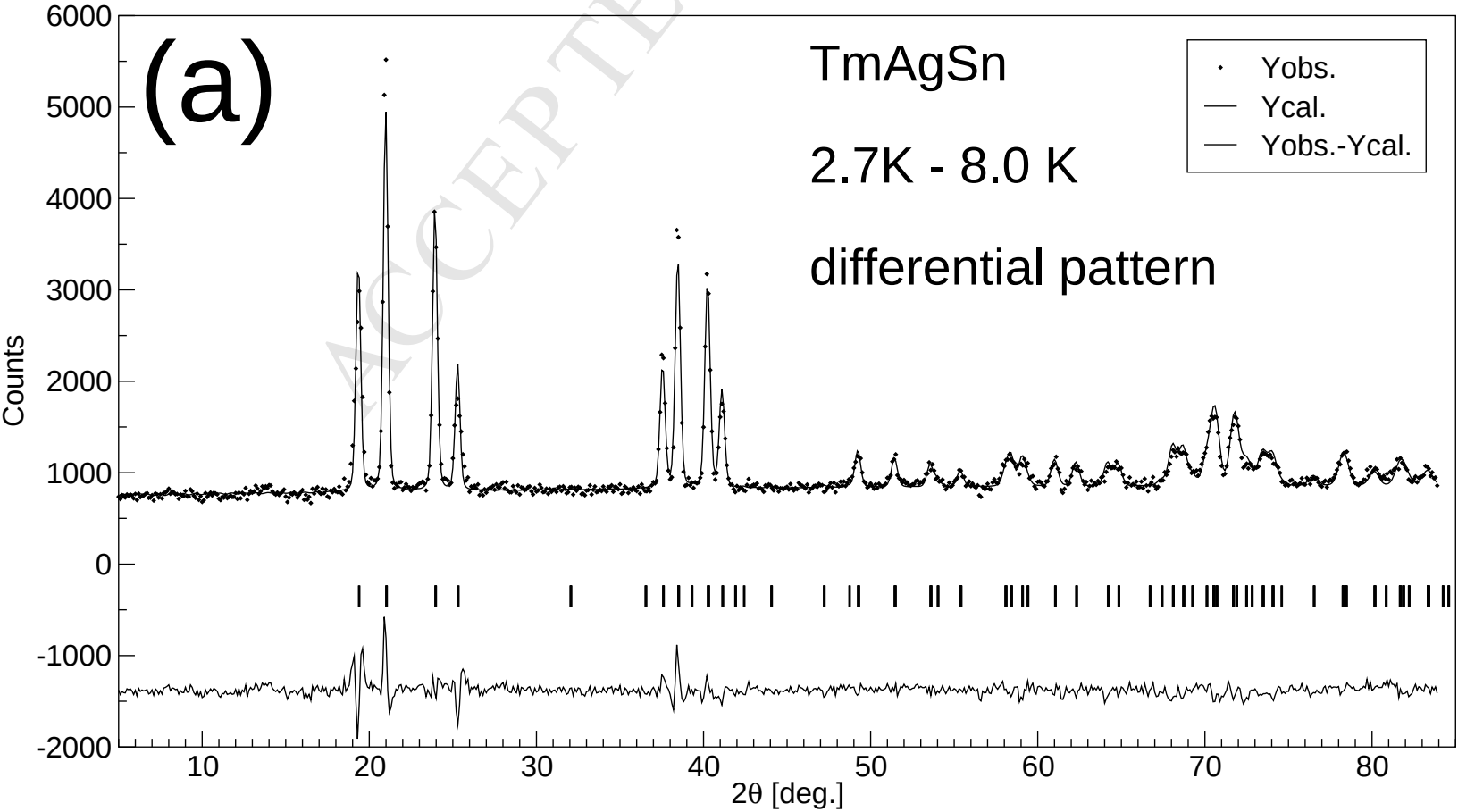

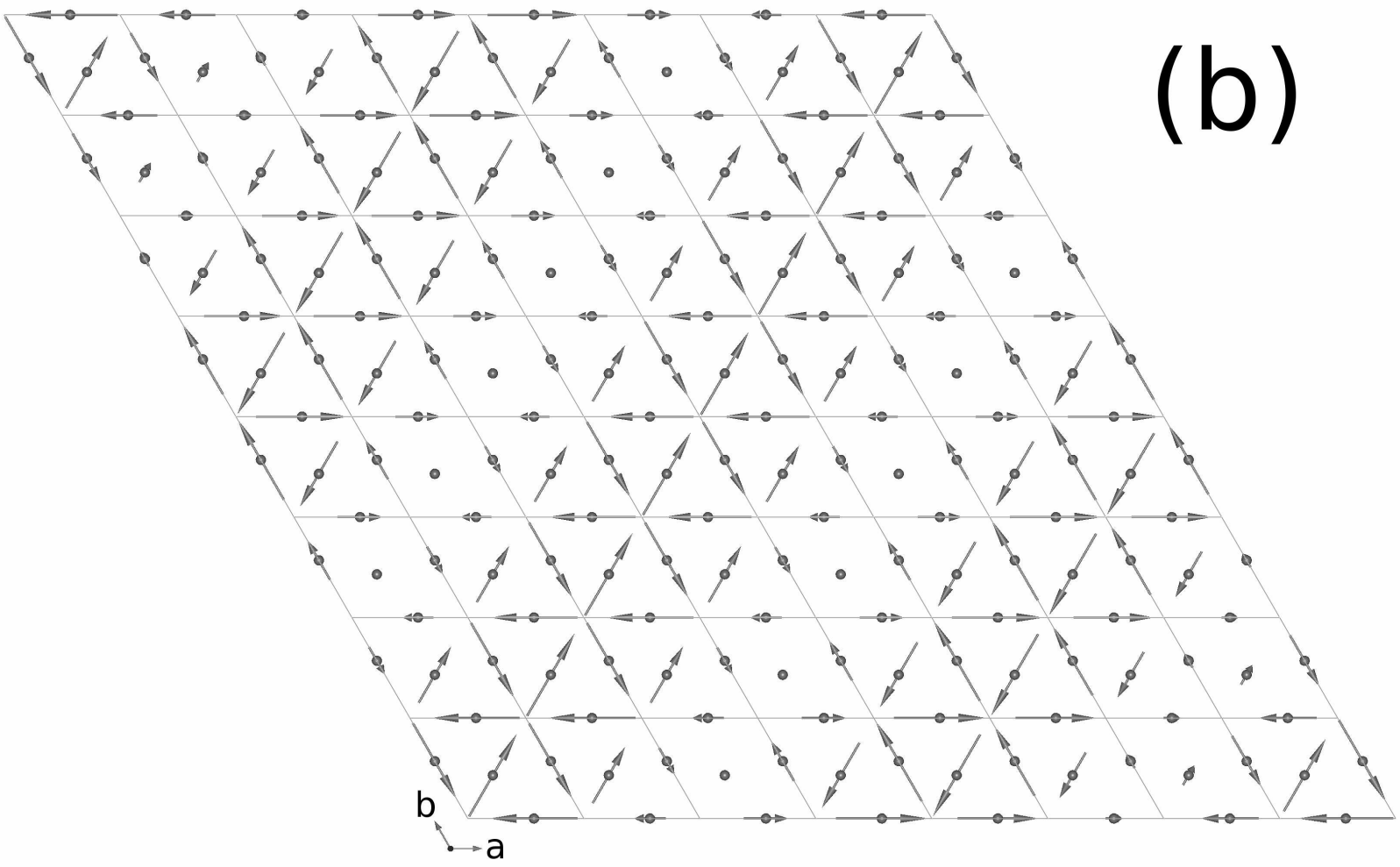
(b)
b
a

Highlights

1) magnetic structures of TmPdIn and TmAgSn are reported for the first time

2) the magnetic structures are verified by group theory symmetry analysis

3) the results are compared with those for other TmTX intermetallics